3rd International Symposium on Particle-image Velocimetry
Santa Barbara, Californai, September 16-18, 1999

QUANTITATIVE VISUALIZATION OF FLOWFIELDS USING TWO-COLOR PIV

S. Gogineni, L. Goss, G. Fiechtner, C. Carter
Innovative Scientific Solutions, Inc.
2766 Indian Ripple Road
Dayton, OH 45440-3638

F. Schauer, J. Gord, and J. Donbar
Propulsion Directorate
Air Force Research Laboratory
Wright-Patterson AFB, OH 45433

Proceedings of the 3rd International Workshop on PIV
Santa Barbara, CA

September 16-18, 1999

QUANTITATIVE VISUALIZATION OF FLOWFIELDS USING TWO-COLOR PIV

S. Gogineni, L. Goss, G. Fiechtner, and C. Carter
Innovative Scientific Solutions, Inc.
2766 Indian Ripple Road
Dayton, OH 45440-3638

F. Schauer, J. Gord, and J. Donbar
Propulsion Directorate
Air Force Research Laboratory
Wright-Patterson AFB, OH 45433

Abstract

The evolution, development, and application of two-color PIV to a wide variety of complex flowfields are discussed, including jet-in-a-crossflow, a supersonic turbulent boundary layer with pressure gradients, flow over a delta wing in a large-scale facility, and vortex-flame interactions. The high-resolution images obtained from these flowfields provide valuable insight concerning the instantaneous nature of the flow and quantitative data that are valuable for developing CFD and combustion models. Two-color PIV is also used simultaneously with planar laser-induced fluorescence (PLIF) imaging for understanding turbulent flame structure.

Introduction

Particle Image Velocimetry (PIV) has been used for a number of years to measure velocity distributions in planar cross sections of aerodynamic flowfields (Adrian, 1991). One of the difficulties involved in implementing this velocimetry technique is the 180-degree directional ambiguity that results from the inability to determine the temporal sequence of the particle pairs. Several techniques have been developed to resolve this ambiguity problem; most involve imposing a shift between consecutive image exposures by means of a scanning or rotating mirror, pulse tagging, a calcite crystal, a polarizing beam splitter, a cross-correlation camera, and color coding of the particles.

The two-color system was originally developed by Goss et al. (1991) for combustion applications and has the following advantages: 1) resolving the directional ambiguity is inherent in the system, 2) higher data yields and signal-to-noise levels are attainable, and 3) the system is suitable for harsh environments and hypersonic flows. In this system two lasers were used--one for producing the green beam (532 nm) and the other for pumping the dye laser to produce the red beam (~ 605 nm); the two beams were combined by a dichroic beam splitter and directed through a set of spherical and cylindrical lenses to generate a laser sheet. The particle images of the flowfield were recorded on 35-mm color film, and the images were analyzed by digitizing the film and using a particle-tracking approach. This technique was applied to several flowfields by Post et al. (1993, 1994) using pulsed lasers as well as a single argon-ion laser. The system was extended to cross-correlation-based PIV (Gogineni et al., 1995) and was applied to a jet-in-a-crossflow flowfield using several seeding strategies.

Unlike single-color PIV systems, extension of the two-color PIV technique from a film-based to a digital-based version was hampered by the lack of commercially available color CCD camera systems. Because of recent developments in color cameras, the difficulty in utilizing color CCD cameras for two-color PIV has decreased significantly. Gogineni et al. (1998) extended film-based two-color PIV to the digital version by recording the color images onto a single, high-resolution, digital (3060 x 2036 pixel) color CCD camera. This digital system was applied to a wide variety of fluid flows such as simulated turbine-film-cooling flows, vortex-flame interactions, turbomachinery flows, a supersonic turbulent boundary layer with pressure gradients, flow over a delta wing in a large-scale facility, and hypersonic flows. Unlike conventional flow-visualization methods, two-color PIV provided images that were useful in analyzing flow structures both qualitatively and quantitatively. These images were also valuable in developing CFD codes. In addition, this system was used for simultaneous velocity and scalar (OH and CH) measurements in turbulent flames (Donbar et al., 1998a and 1998b) and vortex-flame interactions (Fiechtner et al., 1999). Spatial resolution, uncertainty, and sensor performance of this system as compared to color film and Kodak ES 1.0 CCD sensors were also evaluated (Gogineni et al., 1998a, 1999).

Applications

1. Jet-in-a-Crossflow

For understanding the mixing and interaction of a jet and a crossflow, an experiment was conducted by placing the square jet normal to the crossflow (Gogineni et al., 1995). The Reynolds number based on the side of the square jet and the exit velocity of the jet is ~ 600, and the crossflow Reynolds number based on the jet location downstream of the flat-plate leading edge is 9,000. The nominal blowing ratio, defined as the ratio of jet velocity to crossflow velocity, is 1.0. In this experiment a novel approach of seeding the jet and crossflow fluids with different-size particles was used to distinguish the jet fluid from the crossflow fluid.

Figures 1(a) - 1(c) show typical double-exposed two-color PIV images of the jet in a crossflow in the z = 0 plane. Figure 1(a), where only the crossflow was seeded with submicron-size smoke particles, shows the entrainment of the crossflow fluid into the wake region and into jet-shear-layer vortical structures. Figure 1(b), where only the jet flow was seeded with 1-μm Al_2O_3 particles, shows the jet penetration into the crossflow and jet fluid entering the wake region. Although these two images were taken at different instants, they have the same appearance because of the quasi-periodic nature of the flow. In Fig. 1(c) the jet fluid was seeded with 1-μm Al_2O_3 particles, and the crossflow fluid was seeded simultaneously with submicron-size smoke particles in an attempt to understand the interaction of the two fluids. This image enables one to distinguish the jet from the crossflow fluid through the intensity levels of the scattered light (e.g., the bright region corresponds to the jet-flow region, and the dark region corresponds to the crossflow region). These images were processed using cross-correlation procedures, and the resulting velocity distribution for the image of Fig. 1(c) is shown in Fig. 1(d). The vorticity distribution computed from the velocity field was superposed in Fig. 1(d) and clearly shows the shear-layer structures emanating from both the upstream and the downstream lip of the jet. Further details of this study have been reported previously by Gogineni et al. (1998b).

2. Supersonic Turbulent Boundary Layer With Pressure Gradients

A two-color digital PIV (DPIV) system was developed and applied to analyze the structure of a supersonic turbulent boundary layer distorted by wall-curvature-driven streamwise pressure gradients. These tests were performed in a supersonic wind tunnel located at Wright-Patterson AFB. The free-stream Mach number was 2.8 at the measurement location. In this experiment the red laser beam was obtained by passing the green laser beam through a Princeton Optics Model RC1000 Raman cell that contained N_2 and He at a pressure of 65.6 Mpa. Two-color PIV images of the flowfield were recorded using a Kodak DCS 460 CCD camera (3k x 2k pixel array). The performance of this sensor was evaluated by Gogineni et al. (1998a, 1999) using simulated displacements, and the data were found to be in excellent agreement with the corresponding film data and the Kodak ES1.0 data.

Figures 2(a) and 2(b) correspond to zero-pressure-gradient (ZPG) and favorable-pressure-gradient (FPG) conditions. The ZPG boundary-layer structures had an inclination angle of 45 - 60°and spanned approximately one-half the boundary-layer thickness. The FPG boundary layer grew in the streamwise direction, as expected. In addition, a higher population of small-scale structures was evident near the FPG boundary-layer edge, which is consistent with the theory that a FPG promotes the dissociation of large-scale structures into small-scale structures. These images were processed; the mean velocity of the FPG data was compared with the corresponding LDV data obtained in an earlier experiment and found to be in good agreement [Fig. 2(c)]. Further details on this study have been reported by Wier et al. (1999).

3. Flow Over a Delta Wing in a Large-Scale Wind-Tunnel Facility

Several challenges are involved in the transition from small- to large-scale facilities. These challenges include particle illumination and seeding over large regions and recording the particle scattering from a distance far from the selected plane. The ISSI team conducted experiments on the crossflow planes of a delta-wing model (with and without vertical tails) in the Subsonic Aerodynamics Research Laboratory (SARL) wind-tunnel facility at Wright-Patterson AFB. The model was tested at a 23-deg. angle of attack, a Mach number of 0.2, and a Reynolds number of 1.87×10^6 (based on root chord).

Figure 3 shows a two-color PIV image of the flow over a delta wing with tails. The laser-sheet location was at 114.3% root chord. The flowfield was seeded with submicron-size smoke particles. The recording optics were placed 4 m from and at angle of 69 deg. to the illuminated plane. The flow in this case is highly unsteady because of the vortex-bursting phenomenon. The number of secondary structures on the periphery of the primary vortex is higher than that for the flow condition without tails. Figure 3(b) shows the average velocity distribution from eight instantaneous images. These data reveal a counterclockwise vortex motion on the inboard side of the tail. On the outboard side, the velocity vectors mainly follow the direction of the primary vortex motion. The implementation issues regarding this experiment were discussed by Gogineni et al. (1999).

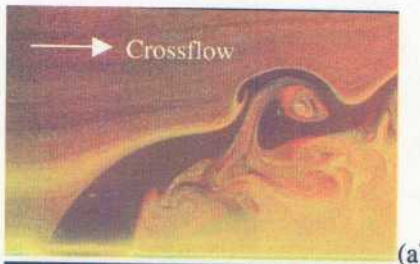

(a)

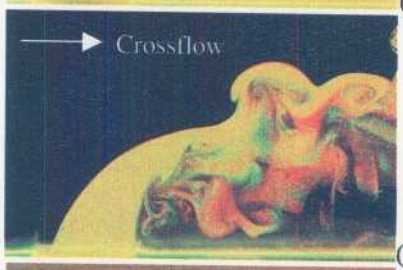

(b)

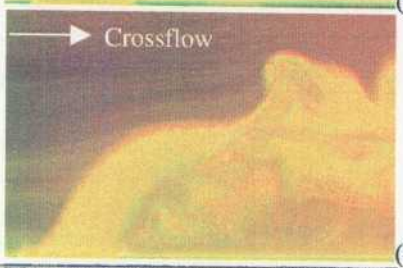

(c)

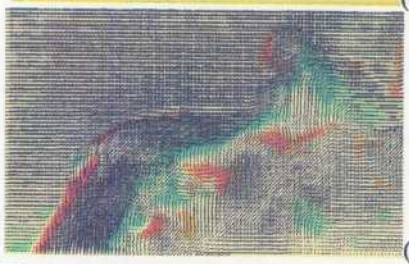

(d)

Fig.1. Flowfield of jet-in-a-crossflow
- (a) Only crossflow seeded
- (b) Only jet flow seeded
- (c) Two seeded simultaneously
- (d) Velocity and vorticity distributions

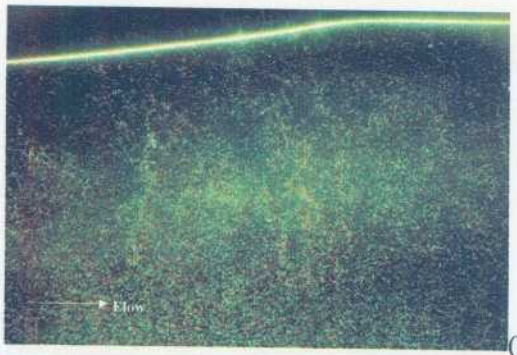

(b)

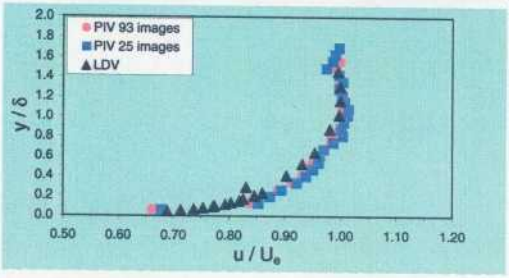

(c)

Fig. 2 Flowfield of supersonic turbulent boundary layer
- (a) Zero Pressure Gradient (ZPG)
- (b) Favorable Pressure Gradient (FPG)
- (c) Comparison of DPIV and LDV data for FPG

(a)

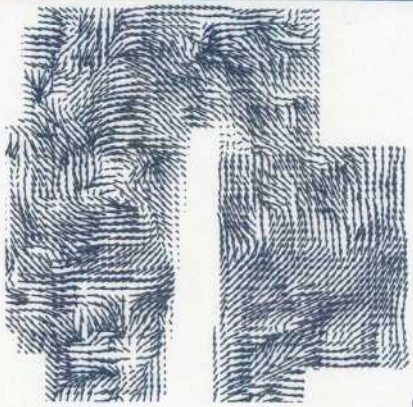

(b)

Fig. 3 Flow over delta wing with vertical tails
- (a) PIV image
- (b) Average velocity distribution

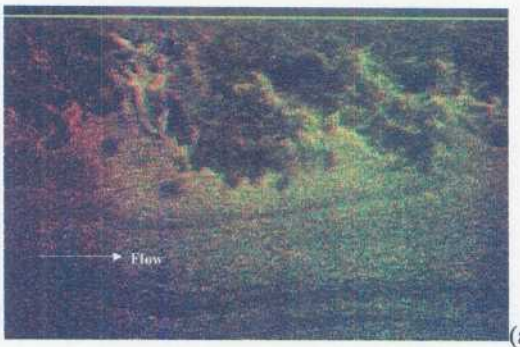

(a)

4. Vortex-Flame Interactions

Vortex-flame interactions in a hydrogen jet diffusion flame were investigated with two-color DPIV and the results used to develop combustion models. Driven-jet vortex-flame interactions are of particular interest because they are reproducible turbulent-like events that can be investigated comprehensively to gain insight into turbulent combustion. Previously, temperature and species-concentration measurements were made in this flame (Hancock, 1996), but a complete understanding of the vortex-flame interactions could not be gained without additional information concerning the flowfield. The vortex structure of the combusting flow could not be reproduced using hot-wire velocity data from cold flows. When the jet-exit velocities from DPIV measurements were used as the driving profile for the DNS code, the resulting computations produced a vortex that matched the experimental vortex (Schauer et al., 1998).

By seeding both the jet flow and the co-flow, Figs. 4(a) and 4(b) were captured for visualizing the entire burner, co-flow, and flame. Figure 4(a) reveals the inner driven fuel-side vortex, the flame-zone where the seed density is low, and the larger flame zone structures above the fuel jet which are produced both by buoyancy and by the periodically driven vortices. It is also evident that the co-flow is effective in producing laminar flow.

In contrast to the driven flame, the undriven flame [Fig. 4(b)] has no inner vortex structure. Figure 4(b) shows a classic jet diffusion flame. Although buoyant structure is evident in this image, it is much different from that in the driven flame of Fig. 4(a), which contains large structures in the flame zone that are much nearer the nozzle. Although not clearly visible in Fig 4(a), a bulge in the flame zone is observed in the driven flame near the inner vortex. The contrasting images show the dramatic effect of the vortex-flame interaction on the overall flame structure.

Figure 5(a) shows a typical DPIV image corresponding to the square region of Fig. 4(a), and Fig. 5(b) displays the velocity and vorticity distributions. The cold-flow image under the same flow conditions is shown in Fig. 6. The difference in vortex structure is attributable to heat-release effects and demonstrates the importance of performing the velocity measurements under reacting conditions for developing combustion models. Figure 7 is a split experimental and computational image of the driven hydrogen jet diffusion flame. The left half is the DPIV image, and the right half is an image from the computational model. The DNS vortex is indicated by theoretical particle traces, and the peak-flame-temperature locations are represented by dots. From Fig. 7 it is evident that the vortex is generated when the faster moving fuel encounters the slower moving fuel, forcing the fuel outward radially and causing a bulge in the flame zone. Similar results are shown in Fig. 7b, which displays the DPIV and DNS images of the cold flow.

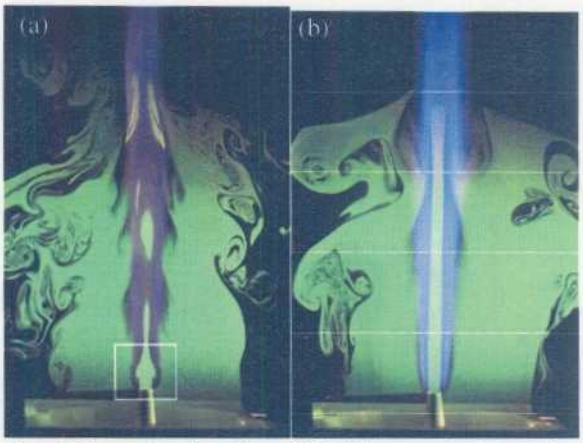

Fig. 4 Flow visualization of (a) driven and (b) undriven hydrogen jet diffusion flame

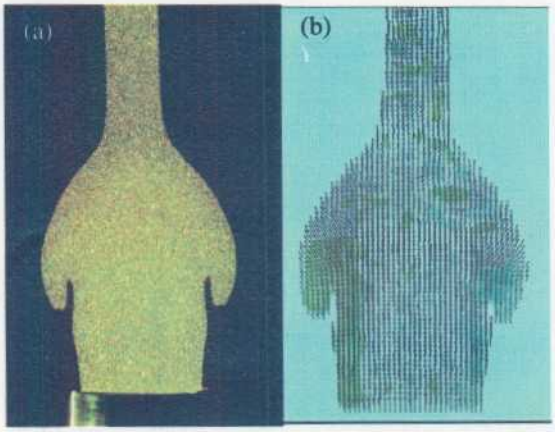

Fig. 5 Flow structure near jet exit (reacting): (a) DPIV image, (b) Velocity superposed with vorticity

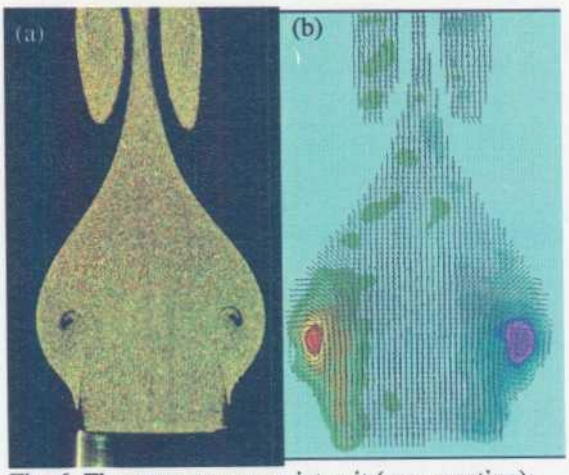

Fig. 6 Flow structure near jet exit (non-reacting): (a) DPIV image, (b) Velocity superposed with vorticity

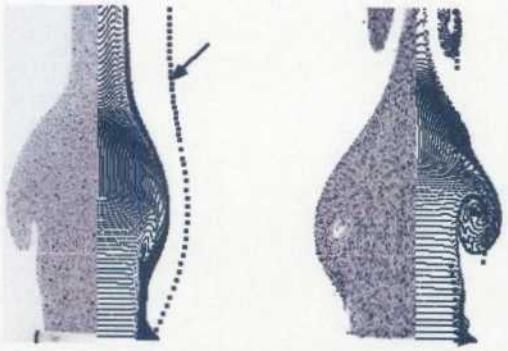

Fig. 7 Split computational and experimental images: (a) Reacting, (b) Non-reacting

The two-color DPIV instrument has also been valuable during recent studies of the interaction of a vortex and a nonpremixed hydrogen-air flame. The vortex was injected into the flame zone of an opposed-jet burner. The images of Fig. 8 were taken using simultaneous planar laser-induced fluorescence (PLIF) of OH (lower half of the figure) and DPIV (upper half of the figure) (Fiechtner et al., 1999). Superimposed on both images is the instantaneous velocity field which, in this case, indicates that the vortex travels upward at 4 m/s. The distinct annular break in the OH layer agrees closely with previous numerical computations of Katta, validating the utility of his CFD code (Katta et al., 1998).

5. Turbulent Flames (Simultaneous Velocity-Scalar Measurements)

Donbar et al. (1998a) addressed the question of whether the chemical-reaction zone within a turbulent, high-Reynolds-number jet flame is thin and can be modeled using strained, wrinkled, laminar flamelet theory or thick and must be modeled using distributed-reaction-zone theory. The region near the wrinkled, instantaneous stoichiometric contour was identified using CH PLIF imaging, and the strain on this interface was measured simultaneously using DPIV. A typical CH PLIF image of a CH_4-N_2-O_2 flame with overlaid vectors is shown in Fig. 9. To visualize the vortical structures, 75% of the mean centerline velocity was subtracted from all vectors; thus, vectors on the low-speed coflow side are pointing downward. Several features of velocity field/CH layer interactions are noticeable, particularly the large structure deforming the top right and the small vortex distorting the middle of the right-hand side of the flame. The upper left-hand side shows a relatively weak CH region that is being influenced by two small vortical structures--one from the jet fluid and the other from the oxidizer. The relative position of the reaction zone and the shear layer is evidenced by the close proximity of the downward-pointing vectors to the CH layer.

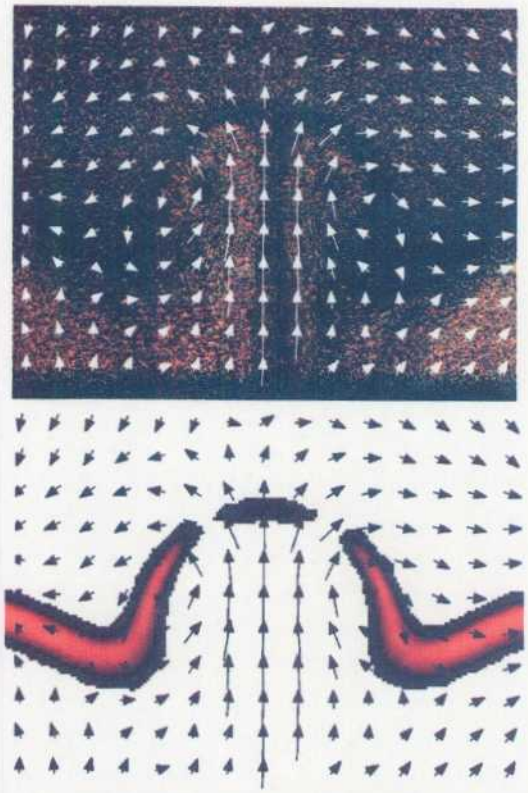

Fig. 8 Interaction of vortex with nonpremixed hydrogen-air flame: (a) DPIV image with velocity vectors, (b) OH PLIF image with velocity vectors

Donbar et al. (1998b) also implemented the simultaneous OH PLIF/PIV technique for characterizing a methane flame diluted with nitrogen, surrounded by a swirling, coflowing mixture of oxygen and nitrogen. Figure 10 shows the realization of the simultaneous OH PLIF/PIV field downstream of the attached diffusion flame. At this position, the flame-front location and structure vary greatly from image to image. This figure shows an unbroken flame, with the velocity field showing little reverse flow in the core region. Near the image center is a vortical structure that has apparently thickened the OH layer in this region. Meanwhile, the flow pattern near the swirl region (lower right edge) has almost wrapped the OH layer back onto itself.

6. Summary

Several complex flowfields were investigated using two-color PIV. The technique proved to be valuable in providing high-quality, high-resolution images. Many of these images were used to develop combustion models and CFD codes. Implementation of this technique for transonic turbomachinery flows and hypersonic flows is currently underway.

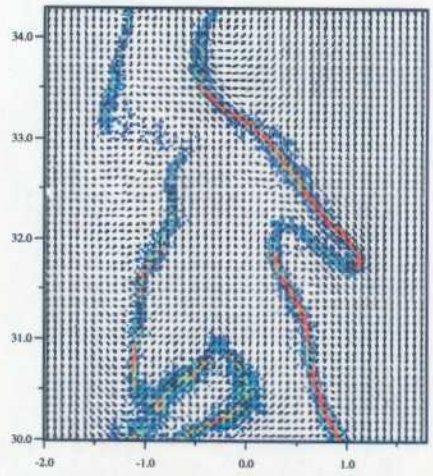

Fig. 9 Simultaneous CH PLIF/PIV image (75% of mean centerline velocity was subtracted from all vectors)

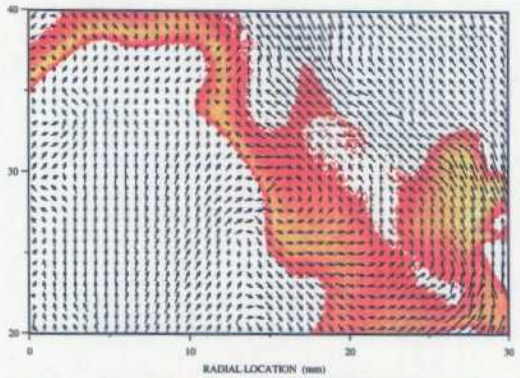

Fig. 10 Simultaneous OH PLIF/PIV image in downstream region of attached diffusion flame

Acknowledgments

This work was supported by the U.S. Air Force Research Laboratory, Propulsion Directorate, Wright-Patterson AFB (WPAFB), OH. The authors would like to thank M. Roquemore, R. Hancock (WPAFB), T. Beutner (AFOSR), R. Bowersox (University of Alabama), and J. Estevadeordal (ISSI) for, experimental assistance and valuable suggestions at various stages of the work. The editorial assistance of M. Whitaker is greatly appreciated.

References

Adrian RJ (1991) Particle imaging techniques for experimental fluid mechanics. Ann Rev Fluid Mech 23: 261-304.

Donbar JM; Driscoll J; Carter, CD (1998a): Simultaneous CH planar laser induced fluorescence and particle imaging velocimetry in turbulent flames. AIAA-98-0151, 36th Aerospace Sciences Meeting and Exhibit, Reno, NV.

Donbar JM; Carter CD; Ratner A; Driscoll J; Dahm J (1998b) Simultaneous velocity-scalar measurements within intensely turbulent non-premixed flames. Fall Technical Meeting, Western States Section of the Combustion Institute, Seattle, WA.

Fiechtner GJ; Renard PH; Carter CD; Gord JR; Rolon JC (1999) Vortex-flame interactions: experimental observation of the annular extinction predicted by Katta. Submitted to Combust Flame.

Gogineni S; Goss L; Sutkus D; Glezer A (1995) Investigation of a jet in a crossflow using PIV. AIAA Paper No. 95-0790, AIAA 33rd Aerospace Sciences Meeting and Exhibit, Reno, NV.

Gogineni S; Goss L; Pestian D; Rivir R (1998a) Two-color digital PIV employing a single CCD camera. Exp Fluids 25: 320-328

Gogineni; Goss L; Roquemore M (1998b) Manipulation of a jet in a cross flow. Exp Thermal Fluid Sci 16: 208-219.

Gogineni S; Goss L; Beutner T (1999) Application of two-color PIV in a large-scale wind tunnel facility. AIAA Paper No. 99-0269, AIAA 37th Aerospace Sciences Meeting and Exhibit, Reno, NV.

Goss LP; Post, ME; Trump DD; Sarka B (1991) Two-color particle-image velocimetry. J Laser Appl 3: 36-42.

Hancock RD (1996) Laser diagnostic investigation of the structure of steady and driven hydrogen jet diffusion flames. Ph.D. Dissertation, University of Illinois, Urbana-Champaign, IL.

Katta VR; Carter CD; Fiechtner GJ; Roquemore WM; Gord JR; Rolon JC (1998) Interaction of a vortex with a flat flame formed between opposing jets of hydrogen and air. Twenty-Second Symposium (International) on Combustion, The Combustion Institute, Pittsburgh, PA, pp 587-594.

Post ME; Goss LP (1993) Two-color particle imaging velocimetry in vortex structures. AIAA-93-0412, 31st Aerospace Sciences Meeting and Exhibit, Reno, NV.

Post ME; Trump DD; Goss LP; Hancock RD (1994) Two-color particle imaging velocimetry using a single argon-ion laser. Exp Fluids 16: 263-272.

Wier R; Bowersox R; Glawe D; Gogineni S (1999) Structure of compressible boundary layer over a curved wall. Submitted to J Prop Power.

Schauer F; Hancock R; Gogineni S; Lucht R (1999) Vortex-flame interactions in hydrogen jet diffusion flames. Submitted to Exp Fluids.